

AD-A283 401



NAVAL POSTGRADUATE SCHOOL

Monterey, California



THESIS

DTIC
ELECTE
AUG 19 1994
S G D

AN ANALYSIS OF THE EFFECTS OF
FEEDLINE AND GROUND SCREEN NOISE
CURRENTS ON A CONICAL MONOPOLE
RECEIVING ANTENNA

by

Thomas D. Gehrki

June, 1994

Thesis Advisor:

Richard W. Adler

Approved for public release; distribution is unlimited

4698

94-26384

DTIC QUALITY INSPECTION



94 8 18 179

REPORT DOCUMENTATION PAGE			Form Approved OMB No. 0704	
Public reporting burden for this collection of information is estimated to average 1 hour per response, including the time for reviewing instruction, searching existing data sources, gathering and maintaining the data needed, and completing and reviewing the collection of information. Send comments regarding this burden estimate or any other aspect of this collection of information, including suggestions for reducing this burden, to Washington Headquarters Services, Directorate for Information Operations and Reports, 1215 Jefferson Davis Highway, Suite 1204, Arlington, VA 22202-4302, and to the Office of Management and Budget, Paperwork Reduction Project (0704-0188) Washington DC 20503.				
1. AGENCY USE ONLY (Leave blank)	2. REPORT DATE June, 1994	3. REPORT TYPE AND DATES COVERED Master's Thesis		
4. TITLE AND SUBTITLE AN ANALYSIS OF THE EFFECTS OF FEEDLINE AND GROUND SCREEN NOISE CURRENTS ON A CONICAL MONOPOLE RECEIVING ANTENNA		5. FUNDING NUMBERS		
6. AUTHOR(S) Gehrki, Thomas D.				
7. PERFORMING ORGANIZATION NAME(S) AND ADDRESS(ES) Naval Postgraduate School Monterey CA 93943-5000		8. PERFORMING ORGANIZATION REPORT NUMBER		
9. SPONSORING/MONITORING AGENCY NAME(S) AND ADDRESS(ES)		10. SPONSORING/MONITORING AGENCY REPORT NUMBER		
11. SUPPLEMENTARY NOTES The views expressed in this thesis are those of the author and do not reflect the official policy or position of the Department of Defense or the U.S. Government.				
12a. DISTRIBUTION/AVAILABILITY STATEMENT Approved for public release; distribution is unlimited.		12b. DISTRIBUTION CODE		
13. ABSTRACT (maximum 200 words) Excessive electromagnetic interference/radio frequency interference (EMI/RFI) degrades the capability of the Naval Security Group (NSG) high frequency direction finding (HFDF) sites to receive signals of interest (SOI). These sites use a circularly disposed antenna array (CDAA) to receive signals in the 2 to 30 MHz frequency range. A conical monopole (CM), an antenna whose bandwidth matches the CDAA's, may provide a solution to the EMI/RFI problem through separation and isolation. Semi-remotely locating the CM away from EMI/RFI sources achieves the former, while its independence from the noisy RF-distribution system accomplishes the latter. This thesis analyzed the susceptibility of the CM to EMI/RFI currents that might be injected onto the feedline from equipment in the building at the center of the CDAA. The Numerical Electromagnetics Code (NEC) was used to model the CM and its buried feedline at the Imperial Beach CDAA site. The numerical model was used to validate proposed limits for the maximum allowable EMI/RFI current on incidental conductors and grounds at receiving sites. A maximum of two microamps of EMI current has been suggested to ensure that no appreciable degradation of SOI reception occurred. The NEC CM model predicted that the two microamp current limit would be adequate for SOI reception on the CM examined. Experimental measurements obtained at the Imperial Beach HFDF site partially validated these results and demonstrated that the CDAA response to the two microamp EMI/RFI limit is within the expected levels.				
14. SUBJECT TERMS Electromagnetic Interference, EMI, Radio Frequency Interference, RFI, Circularly Disposed Antenna Array, CDAA, Conical Monopole Antenna, Receiving Sites.			15. NUMBER OF PAGES 46	
			16. PRICE CODE	
17. SECURITY CLASSIFICATION OF REPORT Unclassified	18. SECURITY CLASSIFICATION OF THIS PAGE Unclassified	19. SECURITY CLASSIFICATION OF ABSTRACT Unclassified	20. LIMITATION OF ABSTRACT UL	

NSN 7540-01-280-5500

Standard Form 298 (Rev. 2-89)

Prescribed by ANSI Std. Z39-18

Approved for public release; distribution is unlimited.

An Analysis of the Effects of
Feedline and Ground Screen Noise Currents
on a Conical Monopole Receiving Antenna

by

Thomas D. Gehrki
Major, United States Marine Corps
B.S.M.E, United States Naval Academy, 1979

Submitted in partial fulfillment
of the requirements for the degree of

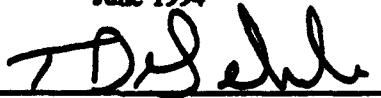
MASTER OF SCIENCE IN ELECTRICAL ENGINEERING

from the

NAVAL POSTGRADUATE SCHOOL

June 1994

Author:



Thomas D. Gehrki

Approved by:



Richard W. Adler, Thesis Advisor



Wilbur R. Vincent, Second Reader



Michael A. Morgan, Chairman

Department of Electrical and Computer Engineering

ABSTRACT

Excessive electromagnetic interference/radio frequency interference (EMI/RFI) degrades the capability of the Naval Security Group (NSG) high frequency direction finding (HFDF) sites to receive signals of interest (SOI). These sites use a circularly disposed antenna array (CDAA) to receive signals in the 2 to 30 MHz frequency range. A conical monopole (CM), an antenna whose bandwidth matches the CDAA's, may provide a solution to the EMI/RFI problem through separation and isolation. Semi-remotely locating the CM away from EMI/RFI sources achieves the former, while its independence from the noisy RF distribution system accomplishes the latter. This thesis analyzed the susceptibility of the CM to EMI/RFI currents that might be injected onto the feedline from equipment in the building at the center of the CDAA.

The Numerical Electromagnetics Code (NEC) was used to model the CM and its buried feedline at the Imperial Beach CDAA site. The numerical model was used to validate proposed limits for the maximum allowable EMI/RFI current on incidental conductors and grounds at receiving sites. A maximum of two microamps of EMI current has been suggested to ensure that no appreciable degradation of SOI reception occurred. The NEC CM model predicted that the two microamp current limit would be adequate for SOI reception on the CM examined. Experimental measurements obtained at the Imperial Beach HFDF site partially validated these results and demonstrated that the CDAA response to the two microamp EMI/RFI limit is within the expected levels.

TABLE OF CONTENTS

I.	INTRODUCTION	1
II	THEORETICAL BACKGROUND	4
	A. POCKLINGTON'S INTEGRAL EQUATION	4
	B. NUMERICAL ELECTROMAGNETICS CODE MODELING GUIDELINES AND ACCURACY	5
	C. CONICAL MONOPOLE OPERATION	7
III.	MODELING THE CONICAL MONOPOLE USING NEC	8
	A. NEC MODELING CONSIDERATIONS	8
	B. NEC RESULTS FOR THE CONICAL MONOPOLE	10
IV.	IMPERIAL BEACH CONICAL MONOPOLE MEASUREMENTS	16
	A. MEASUREMENT TECHNIQUE	16
	B. MEASUREMENTS AND ANALYSIS	17
V.	COUPLING EFFECTS AT IMPERIAL BEACH RECEIVING SITE	25
	A. SITE DESCRIPTION AND COUPLING MEASUREMENT TECHNIQUE	25
	B. COUPLING RESULTS	25
VI.	RESULTS AND CONCLUSIONS	28

APPENDIX A. NEC INPUT DATASET	29
APPENDIX B. FILE CONVERSION PROGRAM	31
LIST OF REFERENCES	35
INITIAL DISTRIBUTION LIST	36

Accession For	
NTIS CRA&I	<input checked="" type="checkbox"/>
DTIC TAB	<input checked="" type="checkbox"/>
Unannounced	<input type="checkbox"/>
Justification _____	
By _____	
Distribution /	
Availability Codes	
Dist	Avail and / or Special
A-1	

ACKNOWLEDGEMENT

To Kristina, who bore the brunt of my anxiety and the lion's share of responsibility in preparing for our move while I completed this thesis.

I. INTRODUCTION

The AN/FRD-10 Wullenweber CDAA is used for signal acquisition and direction finding. When first constructed in the 1960's, this system offered superior detection for low level SOI. Since then the CDAA's capabilities have been significantly degraded by the intrusive effects of EMI/RFI.

Low-level EMI/RFI currents, commonly called noise currents, are produced by a number of sources. Many of these sources have appeared with the advent and widespread use of digital technology. The Naval Postgraduate School's Signal-to-Noise Enhancement Program (SNEP) has identified many of these sources [Ref. 1]. The consequence of EMI/RFI is that previously detectable low level SOI are no longer receivable. One specific reason is that noise currents migrate to the antenna's ground screen and appear at the antenna feedpoint as noise and interference. The noise and interference mask the desired SOI. Extensive CDAA conduction paths consisting of wires, coaxial cables, heating ducts, etc. provide ample opportunities for EMI/RFI currents to travel into other parts of the system and degrade performance. Therefore, it is necessary to limit their magnitude to some acceptable level.

Other NPS SNEP team work [Ref. 2] suggested maximum limits for EMI/RFI currents injected into any conductor,

cable shield, or ground should not exceed two microamps at a small size receiving site. This amount should ensure that the EMI/RFI will be below the ambient noise floor and not affect the reception of a minimum detectible signal level of about -135 dBm. This signal level represents a .002 microamp current at the feedpoint of a 50 ohm antenna.

Through antenna modeling using NEC and field measurements, this thesis examines the relationship between the suggested maximum injected EMI/RFI current and the actual level. Additionally, it analyzes the possibility of limiting the impact of EMI/RFI by semi-remotely locating an antenna far enough away from EMI/RFI sources so noise currents attenuate to acceptable levels before arriving at the antenna feedpoint.

Lemos [Ref. 3] already showed that the CM, an omnidirectional HF antenna, possesses satisfactory radiation receiving patterns in the 2 to 30 MHz operating range. This study will analyze the CM's response to noise currents on its radial ground screen and see if semi-remotely locating it might improve its performance.

Figure 1 provides a side view of the CM and shows one of the 36 radial wires comprising its ground screen. This physical structure is ideally suited for NEC solution methods which employ thin wires to model actual antennas. By exciting the model's structure with current sources, one obtains solutions for the wire currents based on the electric field integral equation (EFIE).

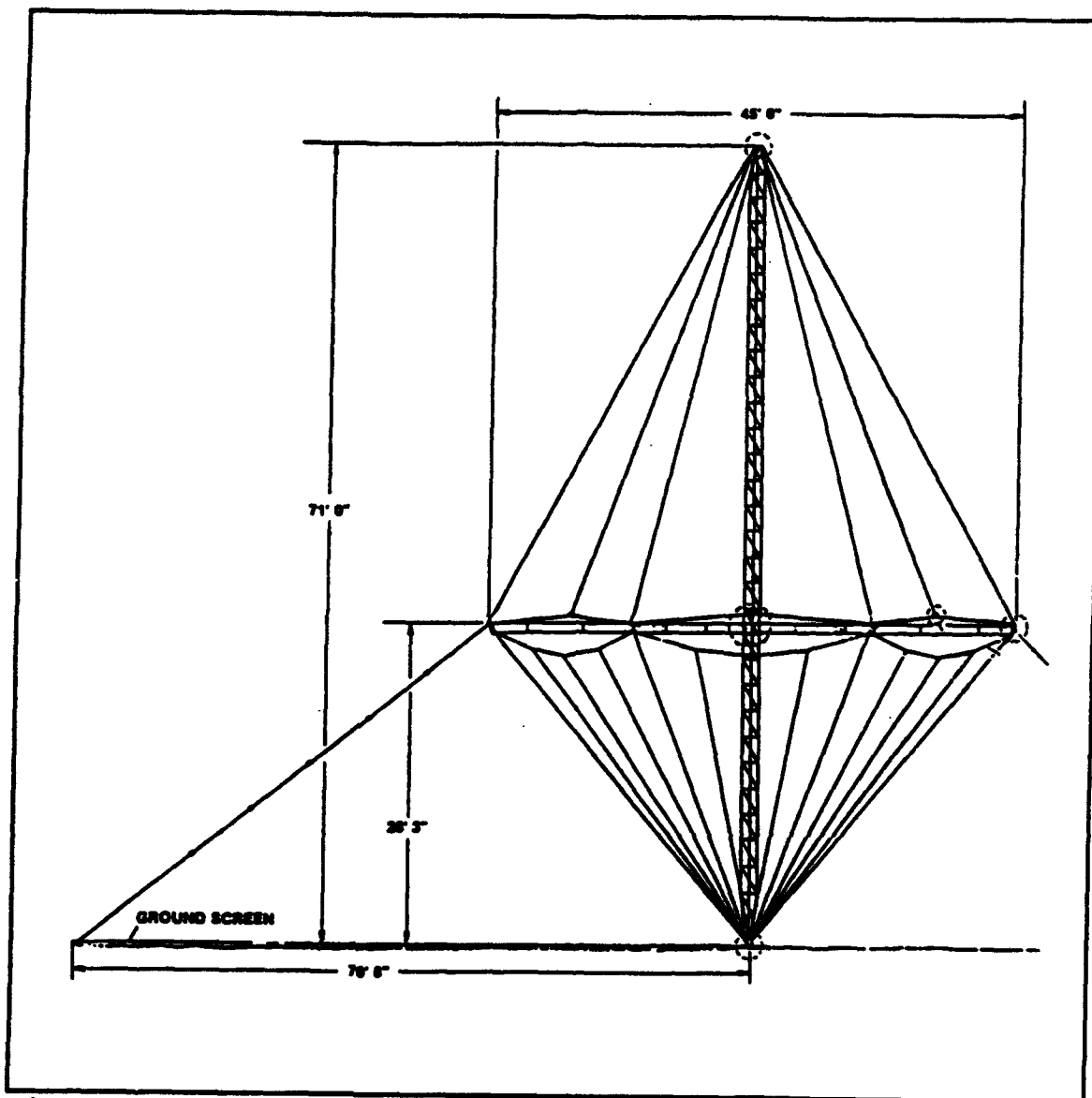


Figure 1. Diagram of the HY-GAIN Conical Monopole [Ref. 3]

II THEORETICAL BACKGROUND

A. POCKLINGTON'S INTEGRAL EQUATION

Balanis [Ref. 4] provides an excellent derivation of the EFIE upon whose theory NEC rests. NEC uses the method of moments, a matrix solution technique, and a special form of the EFIE, known as Pocklington's integral equation, to solve thin-wire antenna problems. Pocklington's integral equation relies on the following four assumptions:

1. Transverse currents are small relative to axial currents on the wire.
2. The circumferential variation in the axial current is small.
3. Current on wires exists as a filament at the center.
4. The boundary condition on the electric field is enforced in the axial direction only.

The EFIE allows computing the radiated field of a wire antenna at any observation point if the current density on the surface of the wire is known. For observation points on the wire, only the axial component on the surface is needed. The thin-wire approximations given above lead to the following scalar integral equation, known as Pocklington's integral equation,

$$-\vec{s} \cdot \vec{E}^i(\vec{r}) = -j \frac{\eta}{4\pi k} \int_c [I(s') (k^2 \vec{s} \cdot \vec{s}') - \frac{\partial^2}{\partial s \partial s'} g(\vec{r}, \vec{r}')] ds' \quad (1)$$

where

$$g(\bar{r}, \bar{r}') = \frac{\exp^{-j\beta|\bar{r}-\bar{r}'|}}{|\bar{r}-\bar{r}'|} , \quad (2)$$

$$k = \omega\sqrt{\mu\epsilon} , \quad (3)$$

and

$$\eta = \sqrt{\frac{\mu}{\epsilon}} . \quad (4)$$

In these equations $I(s')$ is the induced current, E^i is the incident electric field, \bar{s} and \bar{s}' unit vectors tangent to the wire at s and s' , and \bar{r} and \bar{r}' are vectors to the points s and s' on the wire. The electric field is in volts/meter. NEC employs delta weighing functions and special subdomain basis functions known as B spline of the form

$$I_j(s) = A_j + B_j \sin[k(s-s_j)] + C_j \cos[k(s-s_j)] \quad (5)$$

which allow rapid convergence of numerical results [Ref. 5].

B. NUMERICAL ELECTROMAGNETICS CODE MODELING GUIDELINES AND ACCURACY

Burke and Poggio [Ref. 6] provide detailed guidelines on constructing antenna models using NEC. Essentially, by constructing wire models whose segment lengths and diameter

are restricted in terms of wavelength, one ensures numerical accuracy and prevents violating the assumptions associated with Pocklington's integral equation.

For a loss free antenna, average power gain, G_{AVE} , is a check of solution accuracy, and is defined as

$$G_{AVE} = \frac{P_F}{P_I} \quad (6)$$

where P_F is the radiated power in the far field and defined as

$$P_F = \frac{r^2}{2} \lim_{r \rightarrow \infty} \int_{4\pi} \text{Re}[E \times H] \cdot \bar{r} d\Omega \quad (7)$$

and $d\Omega$ is the differential surface on the sphere. P_I is the input power of the antenna given by

$$P_I = \frac{1}{2} \text{Re}(V_I \cdot I_I^*) \quad (8)$$

where: V_I is the input voltage in volts and

I_I is the input current in amperes.

Modeling usually begins by constructing the antenna in free space or over perfect ground, since either situation eliminates the effect of lossy ground on G_{AVE} calculations. In free space, a properly modeled antenna has $G_{AVE} = 1$ while one over perfect ground has $G_{AVE} = 2$. Values within 10% of these ideal averages are usually acceptable.

Realistic antenna problems frequently rely on solutions involving lossy ground. In these cases, NEC uses the Sommerfeld-Norton method [Ref. 6].

C. CONICAL MONOPOLE OPERATION

The CM displays broadband characteristics in the 2 to 30 MHz frequency range. Lemos [Ref. 3] provides a discussion on the characteristics and theory concerning its operation.

III. MODELING THE CONICAL MONOPOLE USING NEC

A. NEC MODELING CONSIDERATIONS

Lemos [Ref. 3] previously validated the model of the CM by evaluating its average power gain over perfect ground in the frequency range of interest. Appendix B contains his NEC input data set with the noticable exception of an added 290 segment wire. This wire attaches to the CM base where the 36 radials join and models a long coaxial cable feedline connecting the CM to a distant CDAA control building.

NEC modeling allows input for real ground's relative permittivity (ϵ_r) and conductivity (σ) in siemens/meter which change significantly with frequency. Figure 2 shows some representative values taken from Hagn [Ref. 7]. Typical values range from extremes for seawater ($\epsilon_r=80$ $\sigma=5$) to those of an urban environment ($\epsilon_r=3$ $\sigma=.001$).

Several methods exist for measuring real ground parameters at antenna sites and should be employed whenever possible to increase the accuracy of the NEC model. Unfortunately, a February winter storm prevented measuring ϵ_r and σ at the Imperial Beach site. Based on measurements taken at other sites and a review of pertinent literature, the model used an ϵ_r of 15 and σ of .003. These values are representative of sandy coastal regions such as southern

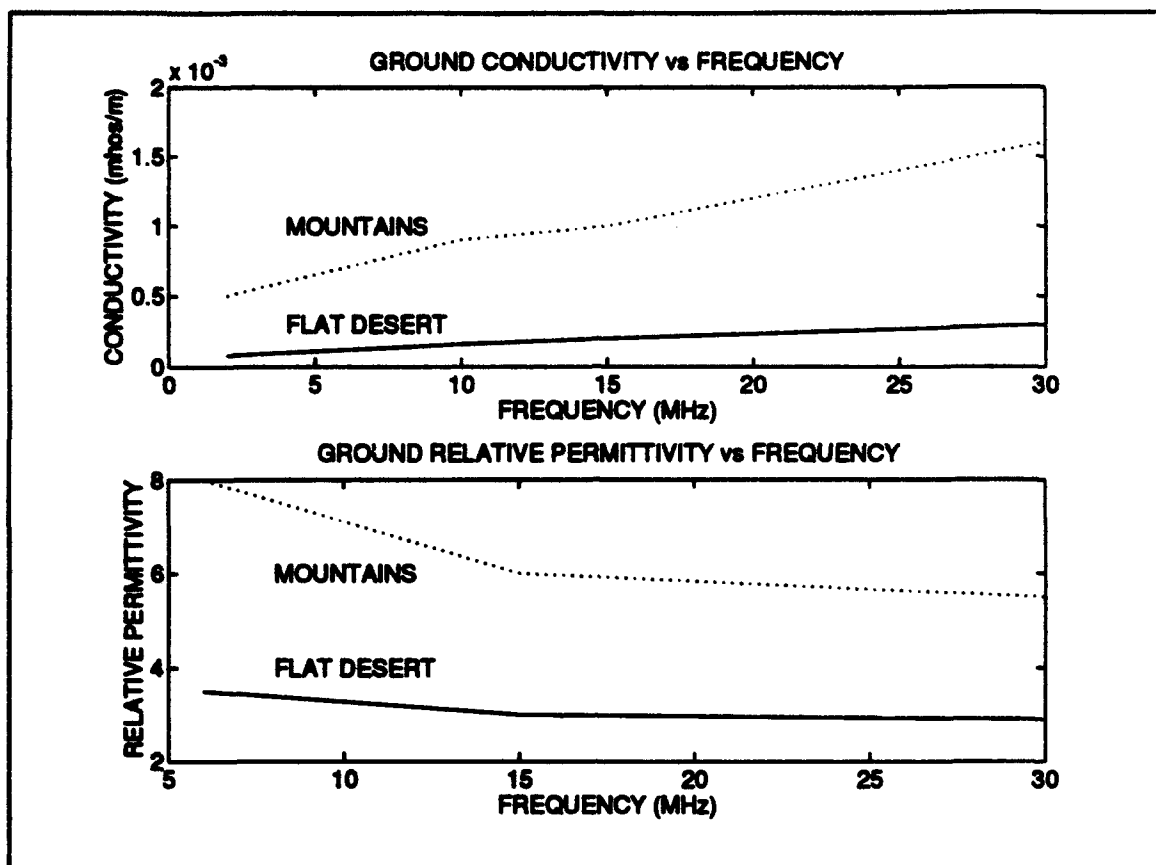


Figure 2. Relative Permittivity and Conductivity Variation with Frequency

California.

To simulate injected EMI/RFI currents, NEC used a 1 amp current source made by connecting an electrically small, poorly radiating element to the antenna model through a network. Since the system is linear, it is possible to scale the results to any convenient value to represent EMI/RFI noise currents.

The primary modeling objective was to simulate EMI/RFI currents coupled onto the shield of a 3200 foot coaxial cable connected to the CM base. This would provide

information about how current attenuates along a coaxial-cable shield as it travels toward the feedpoint of a semi-remotely located CM. Of interest was how far it was from a two microamp source to the location where current drops below the NPS SNEP team's .002 microamp recommended maximum level of feedpoint current. For this model, a current reference source was actually attached 3116 feet from the antenna feedpoint.

A necessary prelude to accomplishing this objective was to validate that the NEC model for the CM accurately predicted feedpoint current levels. An NPS SNEP team devised an experiment to inject current into one of the CM radials and measure the current induced into a 50 ohm resistor at the feedpoint. The NEC predicted results compared very favorably with the experimental values.

B. NEC RESULTS FOR THE CONICAL MONOPOLE

Figure 3 shows the NEC predicted feedpoint current for the CM over the selected frequency range when one radial is injected 42 feet from the feedpoint with two microamps. Several peaks indicate frequencies where strong coupling exists between the radials. The greatest coupling occurs at the 3-MHz peak. Another peak occurs at 10 MHz. Coupling decreases past 10 MHz as the radials become further apart electrically.

Figure 4 shows how the current magnitude and phase

varies for the model along the injected radial at 15 MHz. The linear phase is indicative of a traveling current wave moving in both directions away from the source. The .002 microamp noise floor was plotted to provide a perspective on how this current's magnitude compares to the NPS SNEP team's suggested maximum level of EMI/RFI current at the feedpoint of the CM. Clearly, the injected level of two microamps on the antenna's radial ground screen would significantly interfere with reception of SOI since it is several orders

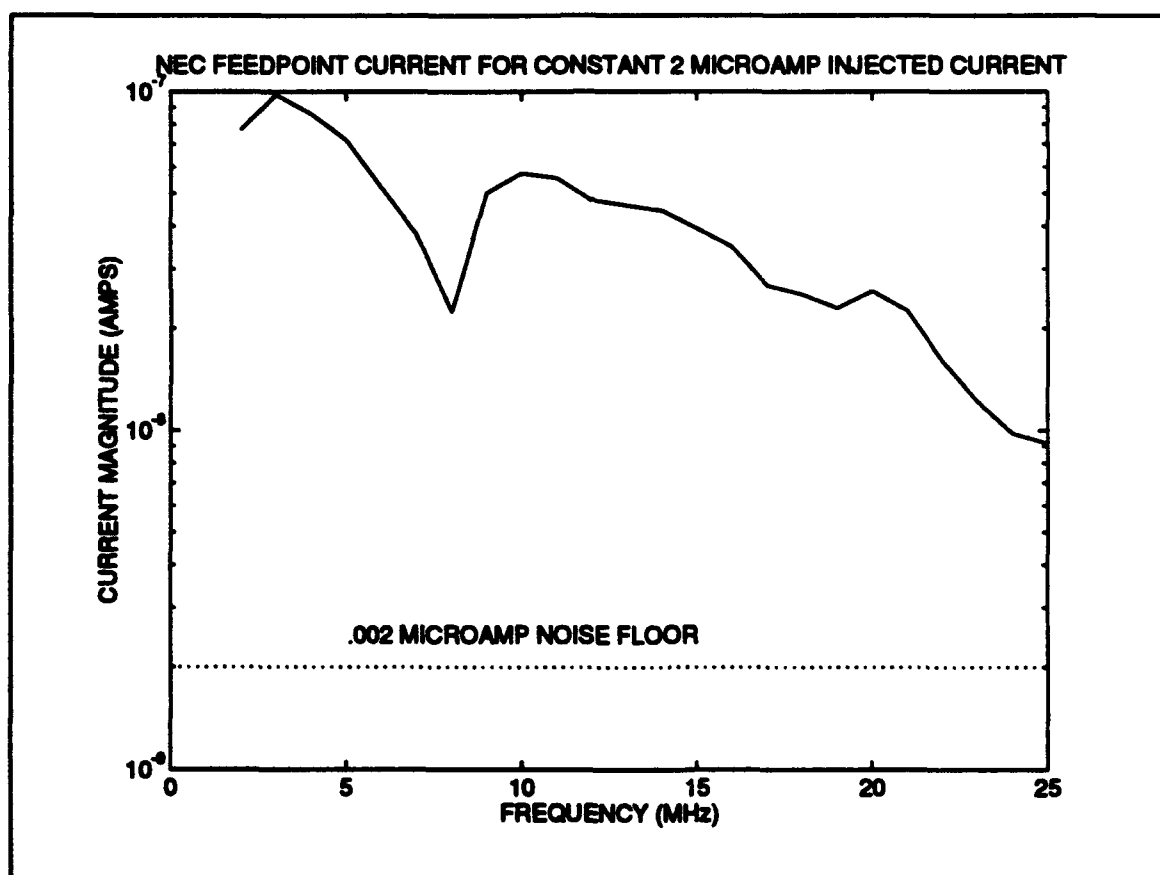


Figure 3. NEC Predicted Feedpoint Current for a Constant 2 Microamp Current Injected into Radial

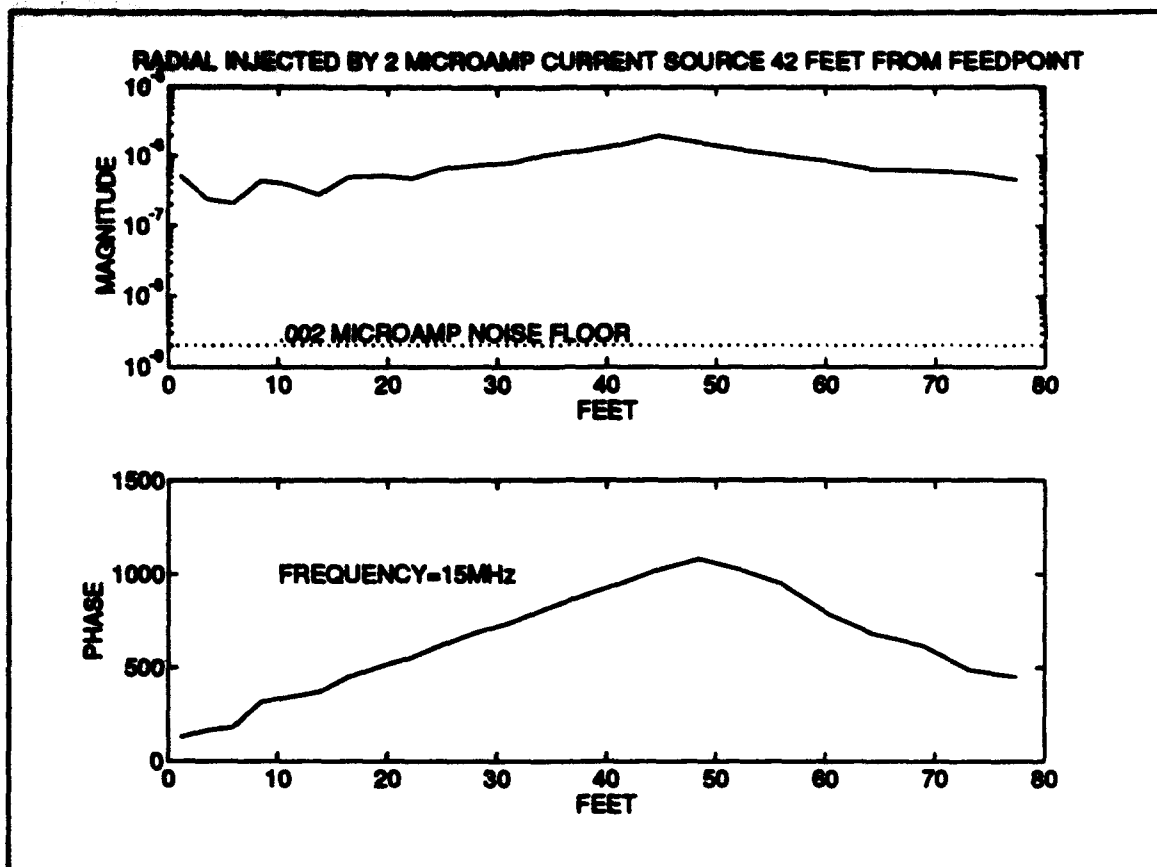


Figure 4. Current Along Radial Wire when Injected 42 Feet from the Feedpoint with 2 microamps at 15 MHz

of magnitude above the ambient noise of a receiver connected to this antenna. Figures 5 and 6 show plots of the current for the case of a 3200 foot wire injected near the end at 3 and 6 MHz respectively. Both cases show that the current rapidly falls off until lateral wave propagation begins about 200 feet from the source [Ref. 8]. After that, a slower but steady attenuation occurs until shortly before the feedpoint, where a number of peaks exist due to reflections from an impedance mismatch occurring at the antenna's base.

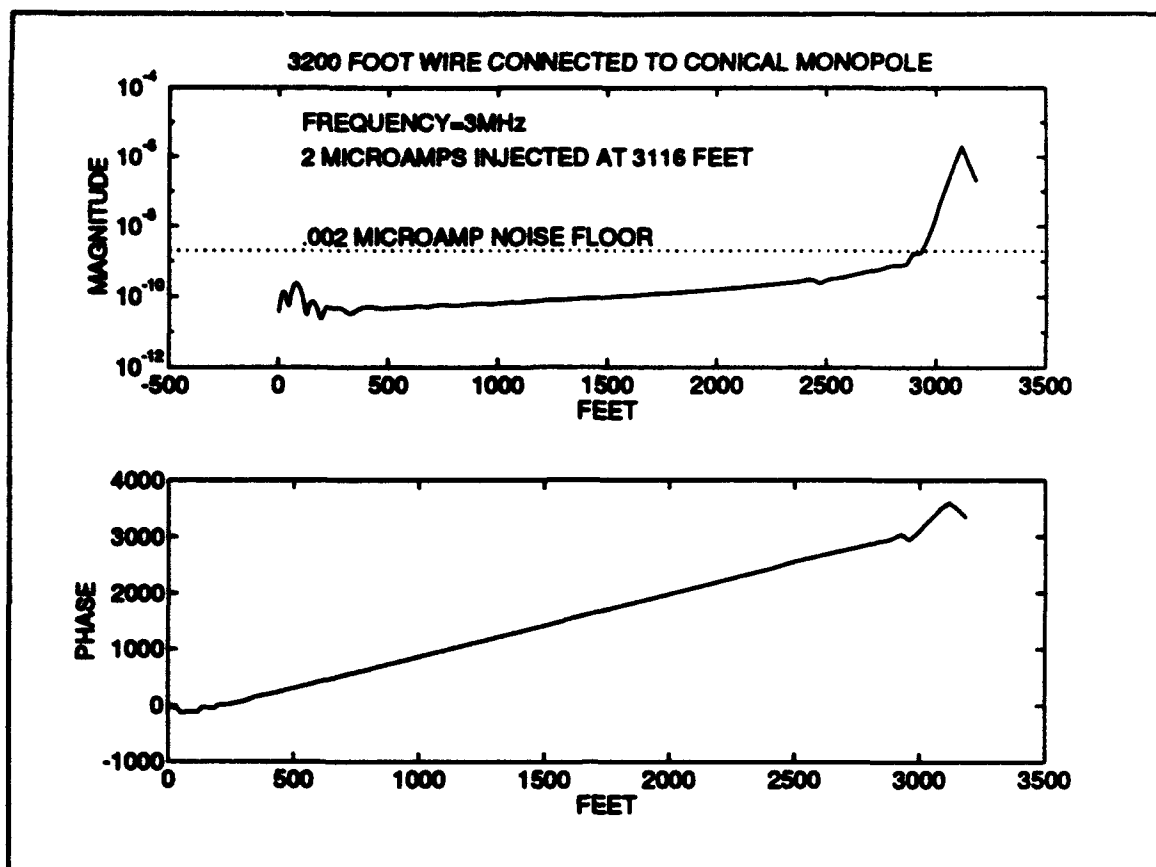


Figure 5. NEC Predicted Current Along a 3200 Foot Coaxial Cable with a 2 microamp Current injected 3116 Feet from the Antenna Feedpoint at 3 MHz

At 3 MHz the current magnitude drops from 2 microamps to below .0001 microamps: a -86 dB attenuation. Since 3 MHz represents the peak coupling frequency, all other frequencies will experience even greater loss.

Table I shows the current magnitude for various distances along the cable. The 3200 foot Imperial Beach CM cable greatly exceeds the length necessary to silence noise sources through attenuation. The shorter cable runs that exist at other CDAA sites with CM antennas, such as 1500 to 2000 feet, would also produce satisfactory attenuation.

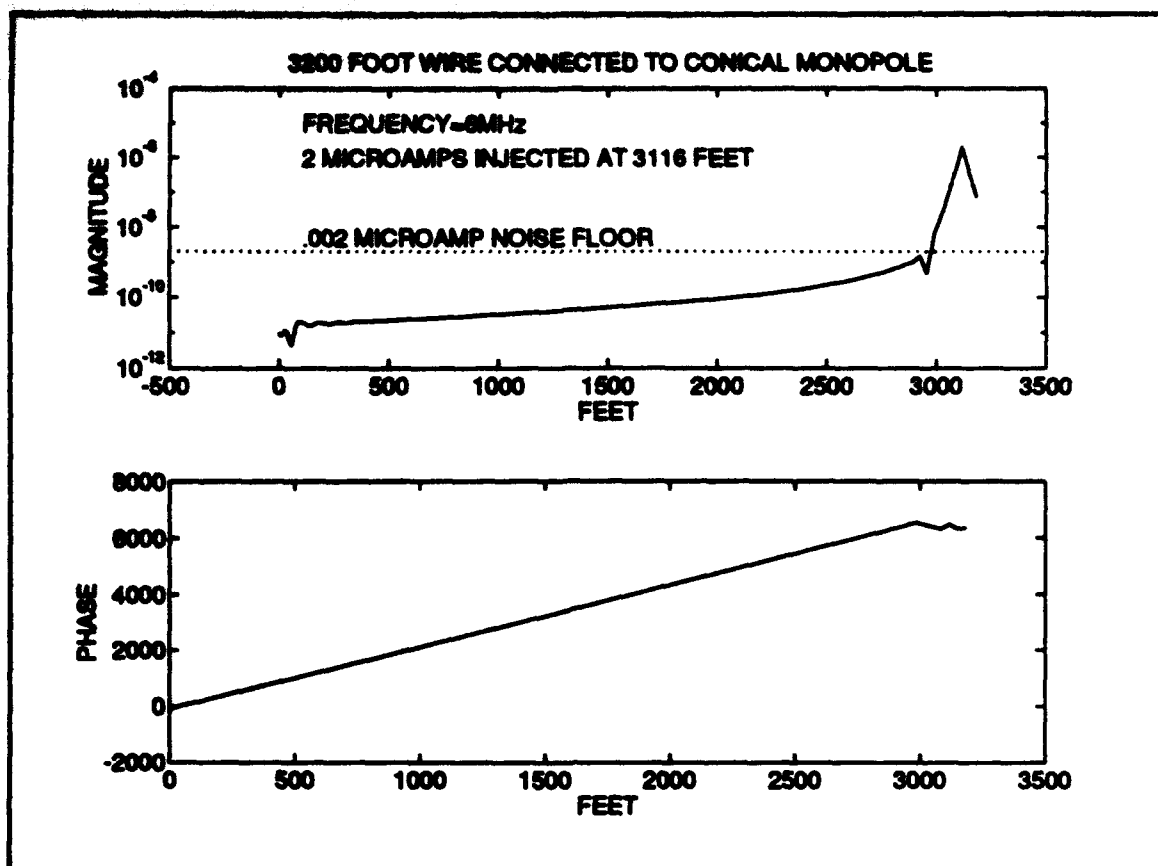


Figure 6 NEC Predicted Current Along a 3200 Foot Coaxial Cable when a 2 Microamp Current is Injected 3116 Feet from the Antenna Feedpoint at 6 MHz

Table I. CURRENT ATTENUATION ALONG 3200 FOOT FEEDLINE FOR 3 AND 6 MHz WHEN INJECTED WITH 2 MICROAMPS AT 3116 FEET

DISTANCE FROM CONICAL MONOPOLE FEEDPOINT	CURRENT MAGNITUDE FOR 3 MHz INJECTION	CURRENT MAGNITUDE FOR 6 MHz INJECTION
FEET	MICROAMPS	MICROAMPS
3116 (INJECTION POINT)	2	2
3083	.62	.35
3051	.175	.082
3018	.048	.017
2988	.01	.006
2956	.0037	.0004
2926	.0016	.0014
2893	.0017	.001
2864	.0008	.0008

IV. IMPERIAL BEACH CONICAL MONOPOLE MEASUREMENTS

A. MEASUREMENT TECHNIQUE

The Imperial Beach CM lies on the coastal plain of southern California characterized by low scrub vegetation and sandy soil. A dense urban environment of mixed residential and industrial zones is within line-of-sight, beginning at three kilometers, and surrounding the antenna on three sides. The ocean, 600 meters away, borders the fourth side.

The CM rises above a circular, six-inch thick gravel carpet which covers its 36 copper radials. Each radial extends 80 feet from the antenna base. Recent maintenance left one six-foot segment of a radial exposed, which provided an excellent location to both inject and measure radial currents. The exposed segment began 40 feet from the base of the CM.

An instrumentation arrangement consisting of a Kenwood Model TS-50 transceiver, 12 dB attenuator, impedance matching tuner, and specially designed signal-injection probe injected current into the radial by inductive coupling. The injection point was 43 feet from the CM base. Placed on both sides, and one foot away, were two Fischer Custom Communications Model F-70 Current Probes. A Hewlett-

Packard 141 Series Spectrum Analyzer, connected to the F-70 probes by low-loss coaxial cable, was used to measure current at the two probe locations as well as the signal level at antenna feedpoint. Figure 7 shows the instrumentation setup. System calibration ensured that 1 microamp of current flowing on a conductor at the F-70 produced an output of 1 microvolt across a 50 ohm load. It was convenient to measure the probe output in dBm dissipated in the 50 ohm load. The following relationship converts the power measured to current.

$$I_{probe} \propto V_{50\Omega} = \sqrt{.001 * 10^{\frac{dBm}{10}} * 50} \text{ (volts)} \quad (9)$$

B. MEASUREMENTS AND ANALYSIS

Table II contains the measured current at both probe locations and the signal level at the CM feedpoint. Several mechanisms account for the significant variation encountered across the 2 to 25 MHz frequency range including:

1. Antenna impedance varies with frequency.
2. Soil permittivity and conductivity parameters vary with frequency.
3. The injecting instrumentation not matching the load equally well at all frequencies resulting in different power levels delivered to the injection coil.
4. Radial/antenna coupling variations with frequency.

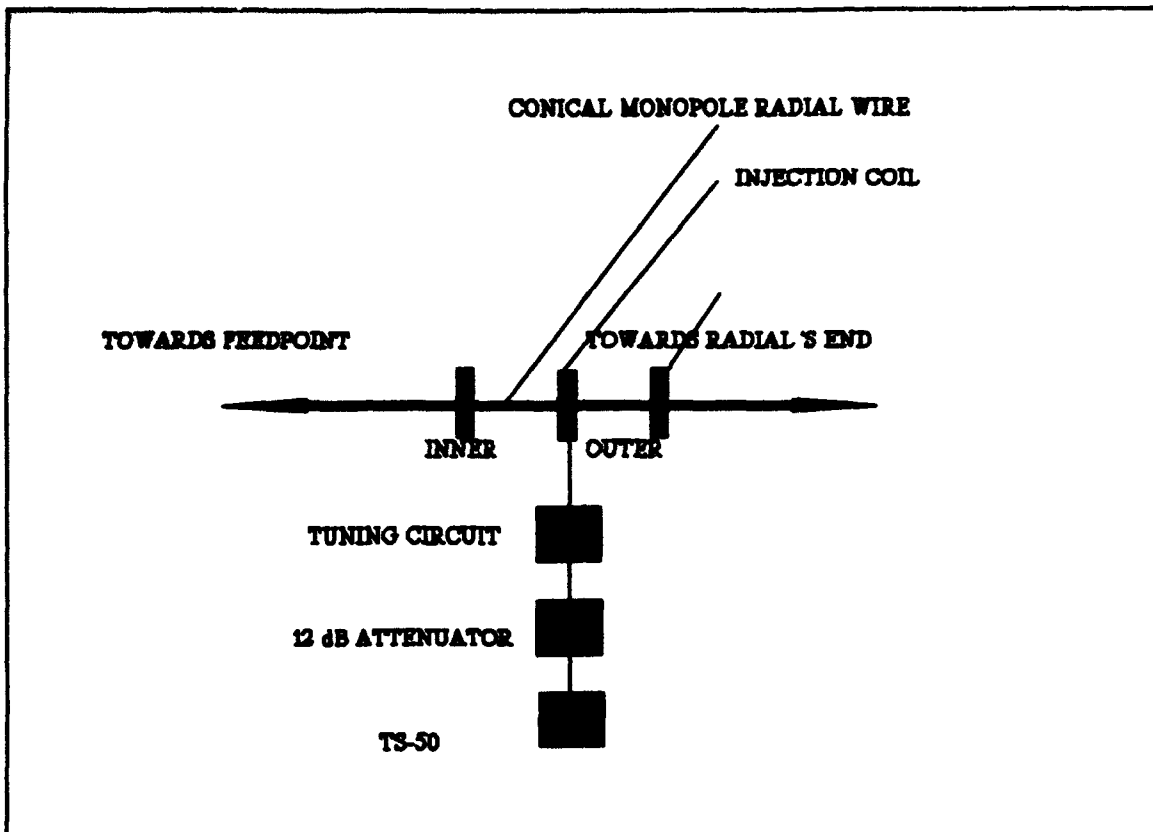


Figure 7. Diagram of Instrumentation Used to Inject and Measure Current on the Conical Monopole

Figure 8 shows the variation of current with frequency at both the inner F-70 probe and the antenna feedpoint. The plot shows a 20 to 40-dB loss between the radial injection point and the measured feedpoint current.

Validating the NEC model results to the actual antenna characteristics requires that the measured and NEC predicted feedpoint currents closely match when both are injected with the same magnitude current at the same location on the antenna.

The NEC values of radial injected current are scaled to be equal to the the measured radial injected current. The

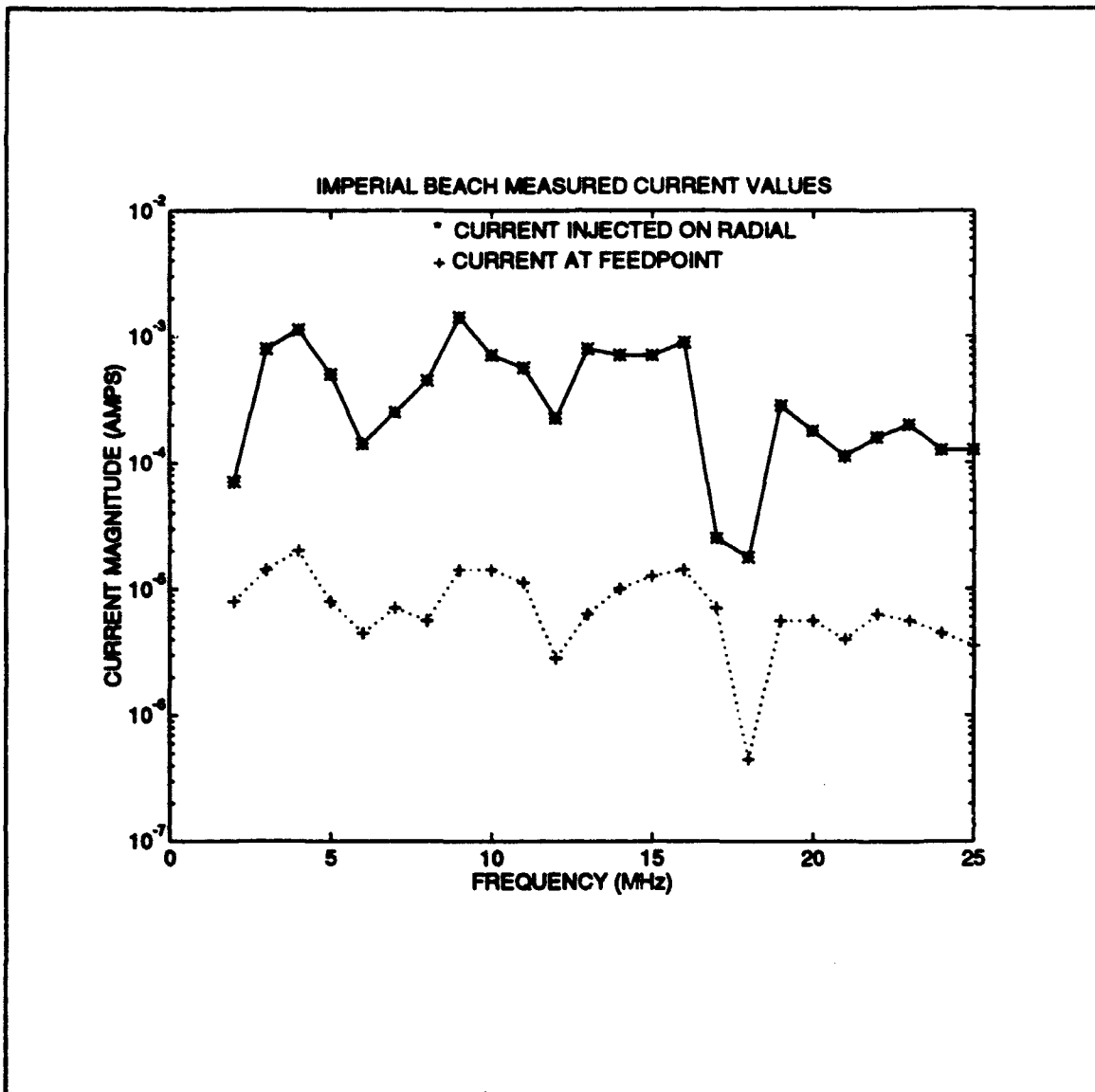


Figure 8. Measured Current at the Inner Probe and at the Conical Monopole Feedpoint

NEC predicted feedpoint current is plotted in Figure 9 along with the measured feedpoint current. The NEC predicted current closely follows the measured current up to about 20 MHz, where the NEC values become consistently lower. A possible explanation is the NEC model used values for ϵ_r and σ that did not change with frequency when in fact there was

Table II. CURRENT ON THE CONICAL MONOPOLE AT INNER AND OUTER PROBES AND AT THE FEEDPOINT

FREQUENCY	CURRENT AT FEEDPOINT	CURRENT MEASURED AT OUTER PROBE	CURRENT MEASURED AT INNER PROBE
MHZ	μ AMPS	μ AMPS	μ AMPS
2	7.95	253	71
3	14.14	705	791
4	19.98	1407	1118
5	7.95	499	449
6	4.47	125	141
7	7.09	223	250
8	5.63	250	445
9	14.14	281	1407
10	14.14	223	707
11	11.23	281	560
12	2.82	141	223
13	6.32	281	791
14	10.01	281	707
15	12.6	100	707
16	14.14	89	888
17	7.07	79	25
18	.45	71	18
19	5.63	79	281
20	5.63	100	177
21	3.99	71	112
22	6.32	63	158
23	5.63	100	199
24	4.47	89	125
25	3.55	71	28

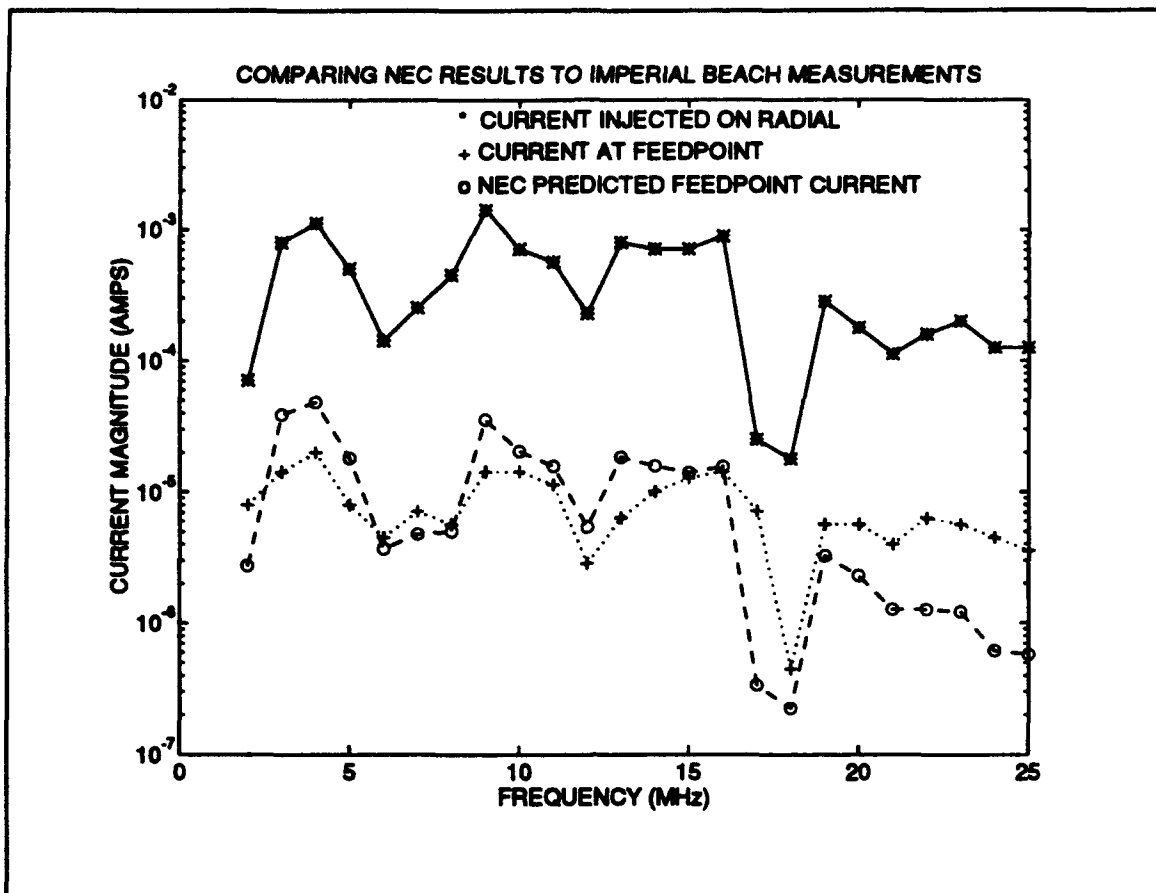


Figure 9 Comparison of NEC Predicted Feedpoint Current to Measured Feedpoint Current for Current Injected on a Radial

some variation. To explore this possibility, the model was run at 22 MHz for a number of different ground parameters. The results are plotted in Figure 10. The solid line in this figure is for the measured value of feedpoint current measured at the Imperial Beach site. Because of the impact of ground constants on the calculated feedpoint current at the higher frequencies, future NEC modeling should employ accurate measurements of ground characteristics.

A final comparison was made between the measured feedpoint current, normalized to 2 microamps, and the NEC

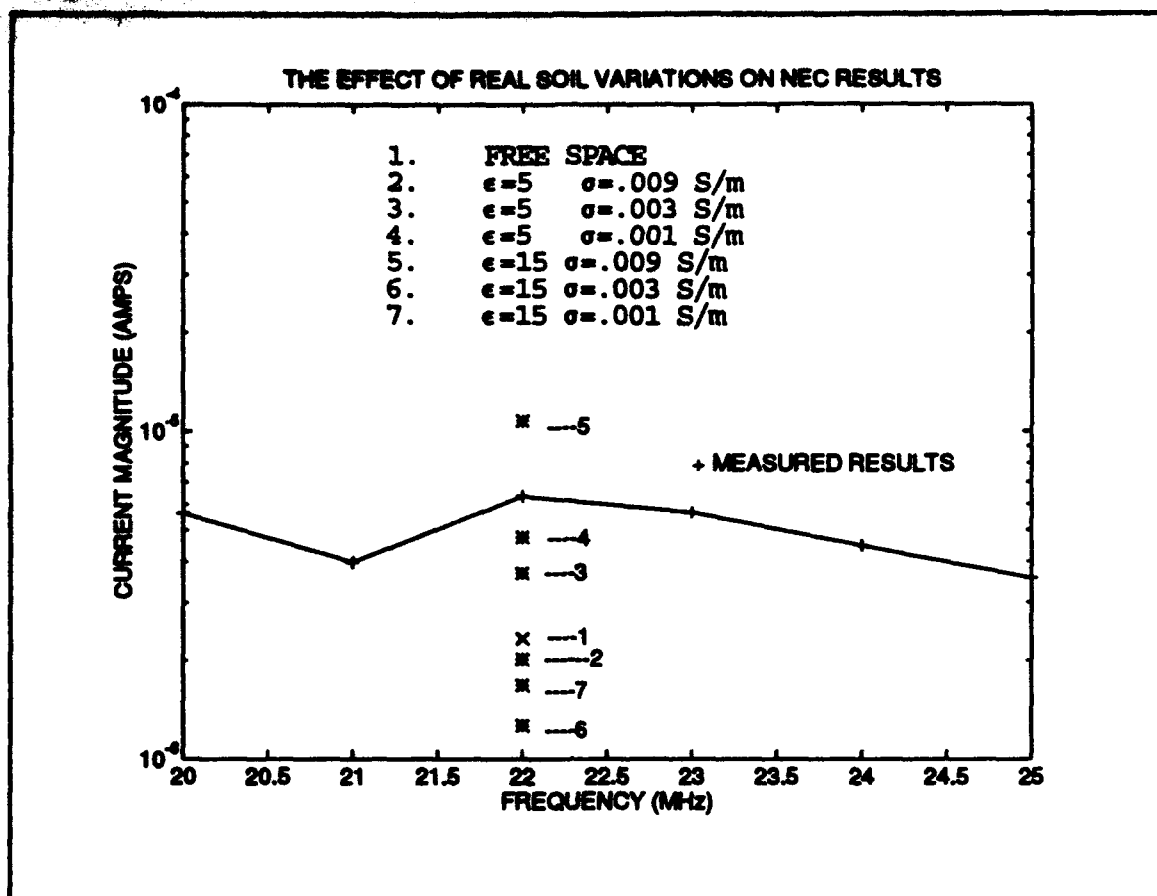


Figure 10. Comparison Between NEC Predicted Feedpoint Current and Measured Feedpoint Current for Varying Ground Parameters

predicted feedpoint current for a 2 microamp injected current. The results, plotted in Figure 11, show close agreement. They diverge above 20 MHz as previously demonstrated. The exceptional peak at 17 MHz, where strong coupling is not expected, needs to be verified. This may be a measurement error.

Now possessing an accurate model, the intent of the NPS SNEP team was to inject current into the CM feedline at various locations and measure the resulting antenna

feedpoint current. This could then be used to verify the numerical results that predict significant attenuation for noise currents traveling along the cable. Regrettably, the Imperial Beach CM feedline had a break in it somewhere between the CDAA operations building and the antenna. This prevented the team from completing this objective. The NPS SNEP team then developed an alternate experiment to test the amount of coupling between coaxial cables that run under an HFDF site.

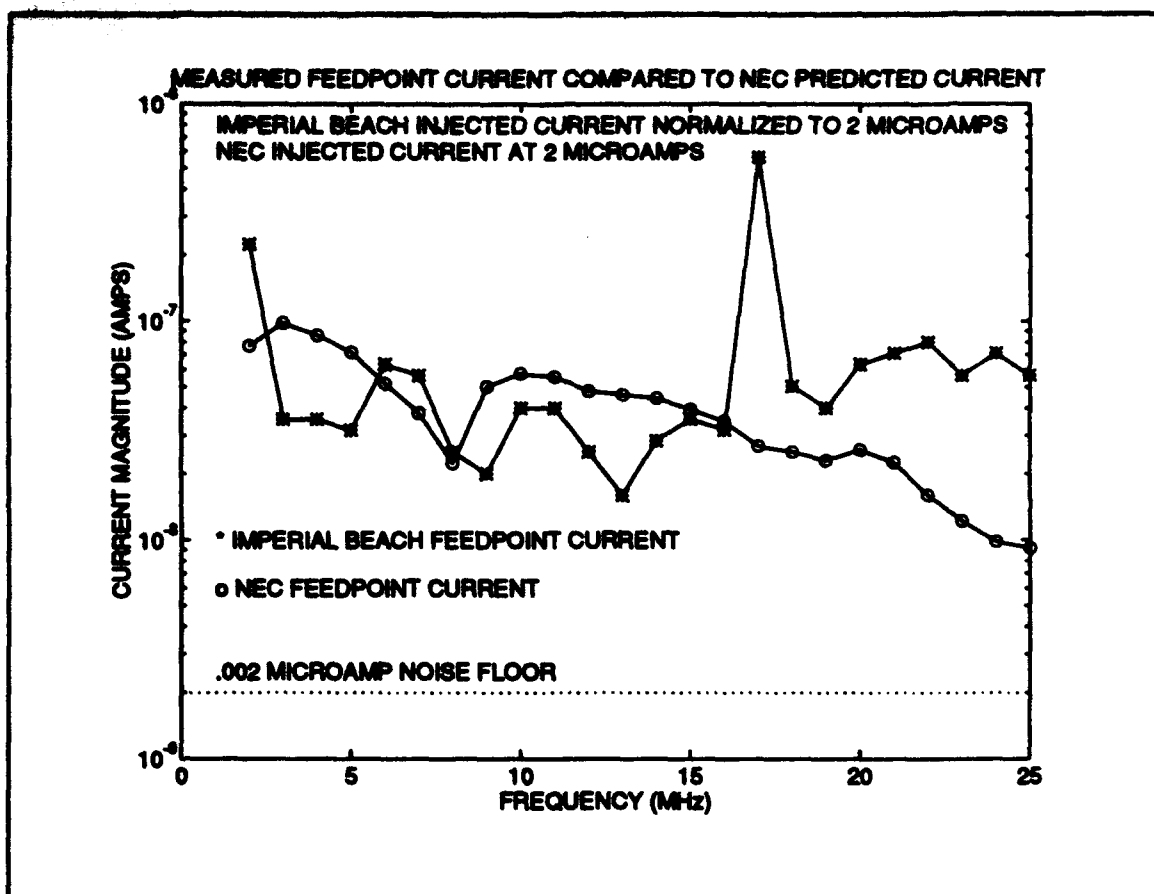


Figure 11. Comparison Between Measured Feedpoint Current and NEC Predicted Feedpoint Current when Radial Injected Current Normalized to 2 Microamps and NEC Radial Injected Current Scaled to 2 Microamps

V. COUPLING EFFECTS AT IMPERIAL BEACH RECEIVING SITE

A. SITE DESCRIPTION AND COUPLING MEASUREMENT TECHNIQUE

The Imperial Beach receiving site consists of the AN/FRD-10 Circularly Disposed Antenna Array (CDAA), control building, and the conical monopole. The latter lies about 3200 feet due north from the control building and is connected by a 7/8-inch-foam dielectric Heliac coaxial cable. Running parallel, and in the same plastic conduit for 270 feet, is a spare CM cable that terminates in an external cable vault. The shield for both cables connect into the north termination plate of the CDAA RF room, where numerous other CDAA cables also connect. For more information, refer to the CDAA technical manual [Ref. 9]. The terrain and soil conditions surrounding the CDAA are similar to at the CM.

An access panel in the RF room of the CDAA allowed the team to select the cables for both current injection and measurement, using the same devices and technique employed on the CM.

B. COUPLING RESULTS

Table III shows the injected and induced current levels in the CM cable shield and spare cable shield, respectively.

Figure 12 shows a plot of the difference in the injected and induced levels and clearly indicates the two cables

Table III. COUPLING VALUES BETWEEN THE CONICAL MONOPOLE CABLE SHIELD AND THE SPARE CONICAL MONOPOLE CABLE SHIELD

FREQUENCY	SIGNAL INJECTION LEVEL	SIGNAL RECEIVED LEVEL	FREQUENCY	SIGNAL INJECTION LEVEL	SIGNAL RECEIVED LEVEL
MHz	dBm	dBm	MHz	dBm	dBm
2	-50	-69	14	-36	-44
3	-37	-44	15	-35	-43
4	-34	-40	16	-36	-44
5	-42	-52	17	-39	-47
6	-54	-75	18	-38	-46
7	-50	-55	19	-40	-49
8	-42	-50	20	-39	-46
9	-42	-51	21	-38	-44
10	-43	-51	22	-54	-54
11	-36	-42	23	-56	-58
12	-38	-46	24	-56	-62
13	-40	-52	25	-60	-76

interact significantly. This serves to dramatically illustrate how noise currents on one conductor couple into adjoining conductors.

The CDAA possesses numerous EMI/RFI conduction paths. Its entire monopole array system resides on a copper ground screen beneath which are hundreds of coaxial cable runs. Added to this are various power conduits, piping systems, and communication cables. Noise current migration is a serious problem in such systems.

This single experiment only touches on the real problem

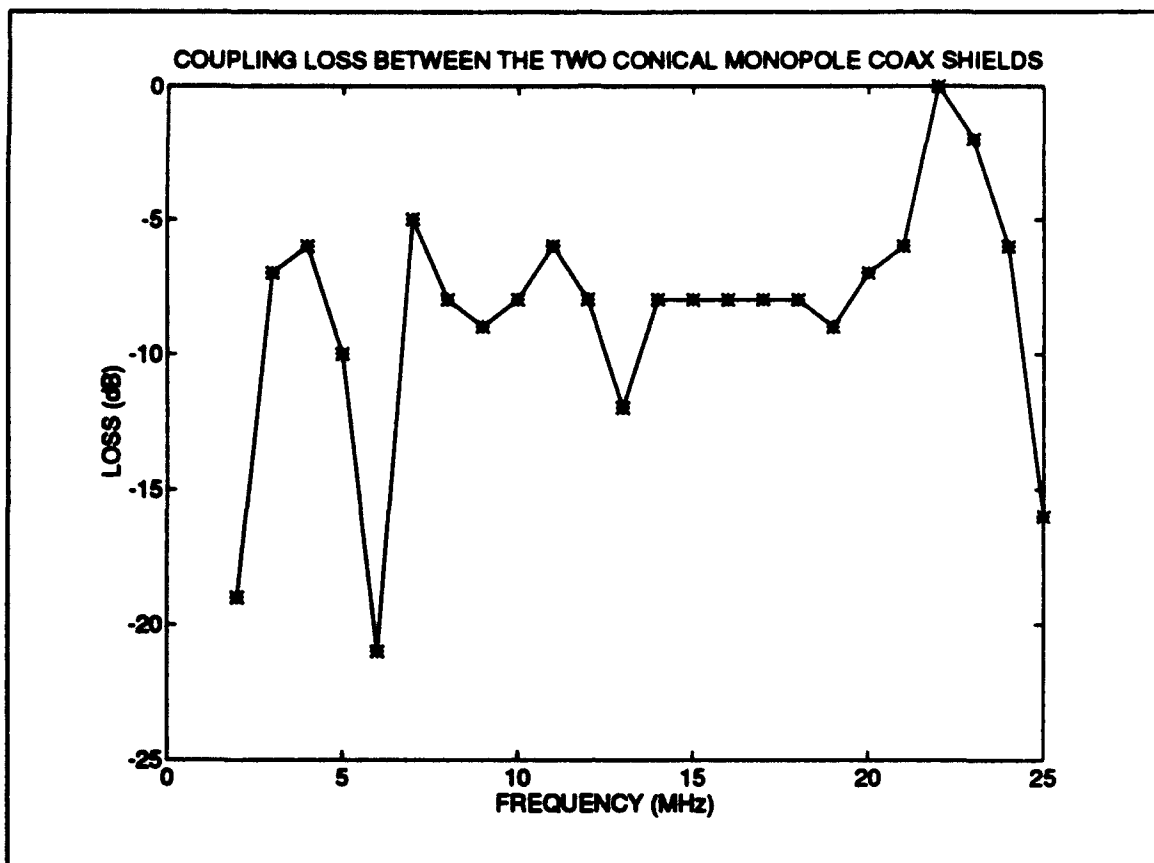


Figure 12. Coupling Between the Conical Monopole Cable Shield and the Conical Monopole Spare Cable Shield

and a detailed analysis of coupling effects between other cables and components awaits. Vincent [Ref. 10] provides other examples of CDAA coupling problems and testing methods. Additionally, he believes coupling testing, if explored further, may provide a relatively easy and inexpensive method to identify transmission line problems such as corroded junctions and incorrectly assembled cables.

VI. RESULTS AND CONCLUSIONS

The NEC model of the CM, with representative values for ground permittivity and conductivity, produced numerical results which closely followed experimental results.

The NEC results also indicate that significant noise current attenuation occurs on the cable shield of a semi-remotely located CM as the current travels on the cable toward the antenna. A distance of 200 feet or more, under Imperial Beach conditions, should reduce this current to levels that will not interfere with HF reception provided the tentative value of maximum injected current of two microamps is not exceeded. These results need to be experimentally verified by injecting an actual CM cable at varying distances from the antenna and measuring feedpoint current levels.

Current injection tests on the coaxial cable sheaths of the CDAA showed the NPS SNEP team proposed two microamp limit on incidental conductors about right [Ref. 10]. Preliminary measurements on coaxial cable shields at the Imperial Beach CDAA site showed that inductive coupling can provide a low-loss path for EMI/RFI currents to travel to other parts of the system. Because of the CDAA's complex network of cables, other experimental tests need to be run. Only then will the full impact of EMI/RFI on the system be better understood.

APPENDIX A. NEC INPUT DATASET

```

CM          THE 2012AA CONICAL MONOPOLE
CM
CM          FROM HY-GAIN TELCONS AND THE MANUAL
CM
CM          FIRST, NECGS RUNS
CM
CM          NO CATENARY/PERF. GND/SIX-FOLD SYMM
CM
CE          ALL EQUI-RADII WIRES
GW 100,16, 0,0,71, 22.5,0,28.5,.01
GW 500,1, 22.5,0,28.5, 18.85,0,28.5, .01
GW 500,6, 18.85,0,28.5, 0,0,28.5, .01
GM 50,1, 0,0,0, 0,0,-1, 500.500
GW 600,1, 18.85,0,28.5, 18.85,0,27.5, .01
GW 200,10, 0,0,.75, 22.5,0,27.5, .01
GM 0,0, 0,0,-30, 0,0,0, 100.600
GW 150,15, 0,0,71, 19.4856,0,28.5, .01
GW 236,14, 0,0,.75, 19.4856,0,27.5, .01
GW 272,14, 0,0,.75, 19.4856,-5.625,27.5, .01
GW 308,14, 0,0,.75, 19.4856,5.625,27.5, .01
GW 400,4, 0,-11.25,0, 0,11.25,0, .01
GM 0,0, 0,0,0, 19.4856,0,28.5, 400.400
GM 50,1, 0,0,0, 0,0,-1, 400.400
GW 800,10, 0,0,-1, 80,0,-1
GC 0,0, 1.25, .01,.01
GM 0,0, 0,0,30, 0,0,0, 800.800
GM 6,5, 0,0,-10, 0,0,0, 800.800
GR 1,6
GS 0,0,.3048
GE -1,2
GN 2,0,0,0,15,.003
FR 0,0,0,0, 6
WG
NX
CE          NOW CALL UP THE NGF FILE
GF
GW 900,1, 0,0,-1, 0,0,0, .01
GW 900,1, 0,0,0, 0,0,.75, .01
GW 900,9, 0,0,.75, 0,0,27.5, .01
GW 900,1, 0,0,27.5, 0,0,28.5, .01
GW 900,14, 0,0,28.5, 0,0,71, .01
GW 902,1, 0,0,-1, 0,0,-2, .01
GW 903,290, 0,0,-2, 3200,0,-2
GC 0,0, 1.01, .01,.01

```

GS 0.0,.3048
GW 901,1, 999,999,999, 999,999,999.001, .00001
GE -1,2
LD 4, 900,2, 2, 50,0,0
NT 901,1, 903,288, 0,0, 0,1, 0,0
EX 0,901,1,0, 0,1
XQ
EN

APPENDIX B. FILE CONVERSION PROGRAM

Compiling this C program produces an executable file called convert.exe that converts NEC generated plotting files into a matrix for MATLAB manipulation.

LCDR Frank Kelbe, an instructor in the Naval Postgraduate School Computer Science Department, authored this program.

```
#include <stdio.h>
#include <alloc.h>
#include <stdlib.h>
#include <string.h>

/* anything longer than this is Part 1 data, shorter
is
Part 2 data */
#define LONG 40

/* if a line is longer than this, the file has
been
converted already */
#define TOO_LONG 70

/* where the real data begins on a line */
#define OFFSET 7

/* length of temp input string */
#define LEN 100

int
main(int argc, char **argv)
{
    FILE *ifp, *fp; /* file
handles */
    FILE *final;

    char tmpfile[LEN]; /*
scratch file name */
    char finalfile[LEN]; /*
scratch
file name */

    char temp[LEN]; /* used
```

```

for
input of strings */
    char temp1[LEN];
/* used
for
input of strings */
    int len;
/*
length of input string */
    char *result;
/*
return
value from fgets */

    if (argc < 2) {
        fprintf(stderr, "\nInvalid number of
arguments.\n");
        exit(1);
    }

    if ((ifp = fopen(argv[1], "r")) == NULL) {
        fprintf(stderr, "\nUnable to open input
file.\n");
        exit(1);
    }

    strcpy(tmpfile, tmpnam(NULL));
/* get a
unique
scratch filename */
    strcpy(finalfile, tmpnam(NULL));
/* get a
unique
scratch filename */

    if ((fp = fopen(tmpfile, "w+")) == NULL) {
        fprintf(stderr, "\nUnable to open output file
%s\n", tmpfile);
        fclose(ifp);
        exit(1);
    }

    while (!feof(ifp)) {
        result = fgets(temp, LEN, ifp);
        if (result != NULL) {
            len = strlen(temp);

            if (len > TOO_LONG) {
                fprintf(stderr, "\n\nThe file
has
already been converted\n\n");
                fclose(ifp);
                exit(1);
            }
        }
    }

```

```

                                if (len > LONG)      { /* proceed only
until
next part */
                                fputs(temp+OFFSET, fp);
                                }
                                else
                                break;                /* quit
when
reach the second part of the data */
                                }
                                }

                                /* open the temp file for reading now */
                                fclose(fp);

                                if ((fp = fopen(tmpfile, "r")) == NULL) {
                                fprintf(stderr, "\nUnable to open temp input
file
%s\n", tmpfile);
                                fclose(ifp);
                                exit(1);
                                }

                                /* open the final output file */
                                if ((final = fopen(finalfile, "w+")) == NULL) {
                                fprintf(stderr, "\nUnable to open output file
%s\n", finalfile);
                                fclose(fp);
                                fclose(ifp);
                                exit(1);
                                }

                                /* temp already has a value, so process
first,
then read more */

                                while (!feof(ifp)) {
                                fgets(temp1, LEN, fp);
                                temp1[strlen(temp1)-1] = '\0';
                                fputs(temp1, final);
                                fputs(" ", final);          /* seperate the
parts
with spaces */
                                fputs(temp+OFFSET, final);
                                if ((result = fgets(temp, LEN, ifp)) == NULL)

                                /* if nothing left, */

                                break;

```



```
/* get out of here */  
}  
  
fclose(ifp);  
fclose(fp);  
fclose(final);  
unlink(argv[1]);  
unlink(tmpfile);  
rename(finalfile,argv[1]);  
return 1;  
}
```

LIST OF REFERENCES

1. Adler, R. W. and Vincent, W. R., "Factors Affecting the Performance of Naval Receiving Sites," paper prepared for the Naval Security Group, San Diego, CA, January 1993.
2. Electrical and Computer Engineering Department Technical Notes, Comments about Electrical Grounds in CDAA Sites, by W. R. Vincent and R. W. Adler, October 1992.
3. Lemos, P. P., *A Computer Analysis of a Conical Monopole for use at Naval High Frequency Receiving Sites*, MS Thesis, Naval Postgraduate School, Monterey, CA, December, 1992.
4. Balanis, C. A., *Advanced Engineering Electromagnetics*, John Wiley & Sons, Inc., 1989.
5. Burke, G. J., "Present Capabilities and New Developments in Antenna Modeling with the Numerical Electromagnetics Code (NEC)," paper prepared for 1985 Tactical Communications Conference, Fort Wayne, Indiana, 3-5 May 1985.
6. Naval Ocean Systems Center Technical Document 116, Volumes (1) and (2), Numerical Electromagnetic Code (NEC) - Method of Moments, by G. J. Burke and A. J. Poggio of Lawrence Livermore Laboratory, January, 1981.
7. Hagn, G. H., "Ground Constants at High Frequencies (HF)," paper presented at the 3rd Annual Review of Applied Computational Electromagnetics, Monterey, California, 24-26 March 1987.
8. King, R. W. P. and Smith, G. S., *Antennas in Matter, Fundamentals, Theory, and Applications*, MIT Press, 1981
9. Space and Naval Warfare Systems Command Technical Manual EE110-SC-MMO-010/W144-FRD10, CDAA Electronic Maintenance (AN/FRD-10), by Quanta Systems Division, 31 August 1987.
10. Engineering Consultant, Technical Memorandum SNEP-940225, *Investigation of EMI Coupling Mechanisms*, by Wilbur R. Vincent, February 1994.

INITIAL DISTRIBUTION LIST

	No. Copies
1. Defense Technical Information Center Cameron Station Alexandria VA 22304-6145	2
2. Library, Code 52 Naval Postgraduate School Monterey, CA 93943-5101	2
3. Chairman, Code EC Department of Electrical and Computer Engineering Naval Postgraduate School Monterey, CA 93943-5121	1
4. Professor Richard W. Adler, Code EC/Ab Department of Electrical and Computer Engineering Naval Postgraduate School Monterey, CA 93943-5121	5
5. Professor Wilbur R. Vincent, Code EC/Ab Department of Electrical and Computer Engineering Naval Postgraduate School Monterey, CA 93943-5121	3
6. Chris Adams ManTech 6593 Commerce Ct. Gainsville, VA 22065	1
7. Roy Bergeron ERA 1595 Spring Hill Rd. Vienna, VA 22180	1
8. Anne M.G. Bilgihan USA INSCOM MSA-V EAQ Bldg 160 MS Vint Hill Farms Warrenton, VA 22186-5160	1
9. Roy Dossat SPAWARS Code PMW 144-3 NC1 3E52, Arlington, VA 20363	1

- | | |
|---|---|
| 10. Jim Engels
NESSEC Code 0411
3801 Nebraska Ave. NW
Washington, DC 20393 | 1 |
| 11. Pamela Guardabascio
NESSEC Code 0411
3801 Nebraska Ave. NW
Washington, DC 20393 | 1 |
| 12. George Hagn
SRI International
1611 N. Kent St.
Arlington, VA 22209 | 1 |
| 13. Clyde Harthcourt
1715 15th St. NW
Washington, DC 20009 | 1 |
| 14. Lee M Jackson
NCCOSC NRAD 825
1918 Via Las Palmas #17
National City, CA 91950 | 1 |
| 15. Leo Jonas
USAF ESC/LEMP
San Antonio, TX 78243-5000 | 1 |
| 16. Sherry M. Jordan
US ARMY INSCOM/MSA-V Bldg160
Vint Hills Farms
Warrenton, VA 22186 | 1 |
| 17. Steve Kelly
NESSEC Code 0411A
3801 Nebraska Ave. NW
Washington, DC 20393-5210 | 1 |
| 18. Brian I. Kutara
NEEACT PAC
Box 130
Pearl Harbor, HI 96860-5170 | 1 |
| 19. CDR Gus Lott
Naval Security Group Command, Code GX
3801 Nebraska Ave. NW
Washington, DC 20393-5210 | 1 |
| 20. Thomas L. Lutz
CC SPAWARSSYSCOM
OMW 169-22 | 1 |

21. Stephen Masison 1
NESSEC Code 0412F
2801 Nebraska Ave. NW
Washington, DC 20393
22. George F. Munch 1
160-CR-375
San Antonio, TX 78253
23. Hugh Myers 1
NEEACT PAC
Box 130 Pearl Harbor, HI 96860-5170
24. LCDR Andrew Parker 1
US Naval Academy
Dept. of Electrical Engr.
Annapolis, MD 21402
25. Jane Perry 1
1921 Hopefield Rd.
Silver Spring, MD 20904
26. Art Reid 1
11177 Bollinger Rd.
Littlestown, PA 17340
27. Miquel I. Sanchez 1
NSA Code G042
Fort Meade, MD 20755-6000
28. Brian Skimmons 1
NSG Code GX
3801 nebraska Ave NW
Washington, DC 20755
29. Miles Terayama 1
NISE West Hawaii
Box 130
Pearl Harbor, HI 96860
30. Tom Watt 1
11443 Rowley Rd
Clarksville, MD 21029
31. Commandant of the Marine Corps 1
Code TE 06
Headquarters, U.S. Marine Corps
Washington, DC 20380-0001

32. Major Thomas Gehrki
3514 Soffit Place
Lake Ridge, VA 22192

3